Precipitation Phenomena in Mixtures of Anionic and Cationic Surfactants in Aqueous Solutions

KEVIN L. STELLNER,[1] JOEL C. AMANTE, JOHN F. SCAMEHORN,[2] AND JEFFREY H. HARWELL

Institute for Applied Surfactant Research, and School of Chemical Engineering and Materials Science, University of Oklahoma, Norman, Oklahoma 73019

Received December 10, 1986; accepted June 15, 1987

The precipitation phase boundary for mixtures of sodium dodecyl sulfate (NaDS) and dodecylpyridinium chloride (DPCl) is determined over a wide range of concentrations. The phase boundary is composed of a monomer–precipitate equilibrium curve, where no micelles exist in solution, and two branches (one NaDS-rich and one DPCl-rich) where monomer, micelles, and precipitate exist in equilibrium. A model is developed to predict the precipitation boundary by combining regular solution theory, to calculate monomer–micelle equilibrium, with a solubility product relationship between surfactant monomer concentrations, to calculate monomer–precipitate equilibrium. Results from the model are shown to work well, except in regions where coacervate formation occurs. An empirical modification to the model is used to account for coacervate formation so that all experimental phase boundaries can be described quite well. The model can also predict the amount of precipitate that will form in any NaDS–DPCl mixture and the results are shown to agree well with experimental measurements.

INTRODUCTION

Considerable work has been done on the interactions between large organic ions with opposite charge in solution. Some of the most important systems include surfactant–dye, surfactant–polymer, and anionic–cationic surfactant mixtures. Surfactant–dye interactions are of interest in pharmaceutical applications where many formulations contain dyes for colorants and surfactants for preservation, solubilization, and stabilization purposes (1–4). Surfactant–dye mixtures have also proven useful in several areas of analytical chemistry (5) including determination of the critical micelle concentration for surfactants (6). Surfactant–polymer systems have been investigated for application in enhanced oil recovery (7–9) and have also found use in hair rinses and conditioners (10–12). Anionic–cationic surfactant mixtures are also of interest in pharmacy (13) and analytical chemistry (14–17), as well as wastewater treatment (18), textile wetting, and detergency (19).

Precipitation is a common phenomenon that can occur in all of the anion–cation mixtures mentioned above, although in most cases precipitation is undesirable because it renders the surfactant ineffective in solution. To understand precipitation in systems such as these, it is necessary to account for processes such as micellization and coacervate formation, which can also occur in solution. In addition, it is important to examine a wide range of anion and cation concentrations so that sufficient information is gathered to provide complete phase boundaries.

To date, the precipitation of anionic surfactant (20–23) and anionic–nonionic surfactant mixtures (24, 25) with simple inorganic cations has been successfully modeled. In this paper, the same type of approach will be used to develop a model for the entire precipitation

[1] Current address: Lever Research Inc., 45 River Road, Edgewater, NJ 07020.

[2] To whom correspondence should be addressed.

0021-9797/88 $3.00

phase boundary of an anionic–cationic mixed surfactant system. This anionic–cationic mixture is the simplest of the systems introduced here because both species are surface active and their solution chemistry is well defined (i.e., mixed micelle formation). In surfactant–dye and surfactant–polymer systems, however, one component is not surface active, so smaller aggregates (5, 26, 27) or pseudomicelles (1) may form which may be more difficult to account for. It should be possible to modify the model presented here to include these types of interactions so that a more generalized model would result.

EXPERIMENTAL

Materials

The anionic surfactant used is sodium dodecyl sulfate (NaDS), obtained from Fisher Scientific, which was recrystallized twice from a 50/50 mixture of water and ethanol then dried under vacuum with low heat. The cationic surfactant is dodecylpyridinium chloride (DPCl) which was received as technical grade from Pfaltz and Bayer. This was recrystallized three times from an approximately 80/20 mixture of petroleum ether and ethanol and the crystals were dried under vacuum with low heat. Neither surfactant showed a minimum in surface tension curves and no impurities were observed using high-performance liquid chromatography with a conductivity detector. The NaCl (Fisher certified) was used as received and the water was distilled and deionized.

Methods

To determine a point on the precipitation phase boundary, a series of solutions were prepared (in 100-ml volumetric flasks) each containing a constant amount of NaDS, 0.15 *M* added NaCl, and varying amounts of DPCl. Surfactant solutions can remain supersaturated for long periods of time before precipitation is complete (22); therefore, all solutions were cooled to force precipitation to occur. The solutions were then placed in a water bath at 30.0 ± 0.1°C, shaken periodically, and allowed to equilibrate for at least 4 days before determinations were made. If a solution was outside of the precipitation region, crystals would dissolve so that the solution became isotropic. If crystals remained in solution after equilibration, the initial solution composition was considered to be inside the precipitation region. Using this procedure, the boundary of the precipitation region could be determined and in all cases, for a given NaDS concentration, the concentration of DPCl that determined a point on the boundary was accurate to within ±10%.

Several techniques were used to detect the presence of precipitate in solutions. In most cases, the phase boundary can be determined accurately by simple visual inspection. However, at low concentrations, where only a small amount of precipitate forms, it is very difficult to see any crystals. A 4 mW helium neon laser (Spectra Physics) was used to obtain more accurate phase boundaries by passing the beam through a series of solutions. At an observation angle of 90° to the incident beam, scattering of the beam was clearly evident in some solutions, indicating the presence of small particles (21, 28).

Another technique used to determine the location of the phase boundary at low surfactant concentrations was a dodecyl sulfate anion selective electrode (Roth Scientific) which responds only to free anionic surfactant ions in solution. When electrode response (relative millivolts) is plotted versus increasing DPCl concentration for a series of solutions with constant NaDS, a break occurs at the lowest DPCl concentration where precipitate is present. Similarly, a UV spectrophotometer (Bausch and Lomb) was used to detect monomeric dodecylpyridinium cations in solution. Therefore, for a series of solutions with constant DPCl and increasing NaDS concentration, a break in the plot of absorbance (at 255 nm) versus NaDS concentration indicated the solution in which precipitation first began to occur. In these experiments, suspended particles must be eliminated because they will

cause erroneously high absorbance readings. This is accomplished by centrifuging each solution for 30 min and allowing them to re-equilibrate at 30°C for 24 h before absorbance is measured.

Surface tension measurements were used to determine the critical micelle concentration (CMC) of each pure surfactant in 0.15 *M* NaCl by a break in the curve of surface tension versus logarithm of surfactant concentration. A DuNuoy ring tensiometer (Central Scientific) with a platinum–iridium ring was used and all the necessary precautions were taken to maximize accuracy (29). Solutions were allowed to equilibrate at 30°C until surface tension readings stabilized. Equilibration times ranged from 15 min for concentrated solutions to 3.5 h for dilute solutions.

An elemental analysis of the dodecylpyridinium–dodecyl sulfate precipitate was performed by Huffman Laboratories (Wheat Ridge, CO). The sample was prepared by filtering crystals from several solutions, washing with cold water to remove excess NaCl, and drying under vacuum with low heat.

THEORY

When small amounts of anionic and cationic surfactants are added to an aqueous solution, they completely dissociate and exist only as ionic monomers. As surfactant concentration is increased, micelles begin to form when the CMC is reached. If the monomer concentrations of anionic and cationic surfactant exceed the solubility product, precipitate will form. There are two basic equilibria, therefore, that must be considered in solutions of anionic–cationic surfactant mixtures: monomer–micelle equilibrium and monomer–precipitate equilibrium. The schematic diagram in Fig. 1 demonstrates this point.

As shown in Fig. 1, the anionic and cationic surfactants can be present in three environments: as monomer (unassociated molecules); incorporated in mixed (anionic plus cationic) micelles; and as precipitate. The counterions (Na^+ and Cl^-), which have been excluded from Fig. 1 for clarity, can be bound onto the micelle

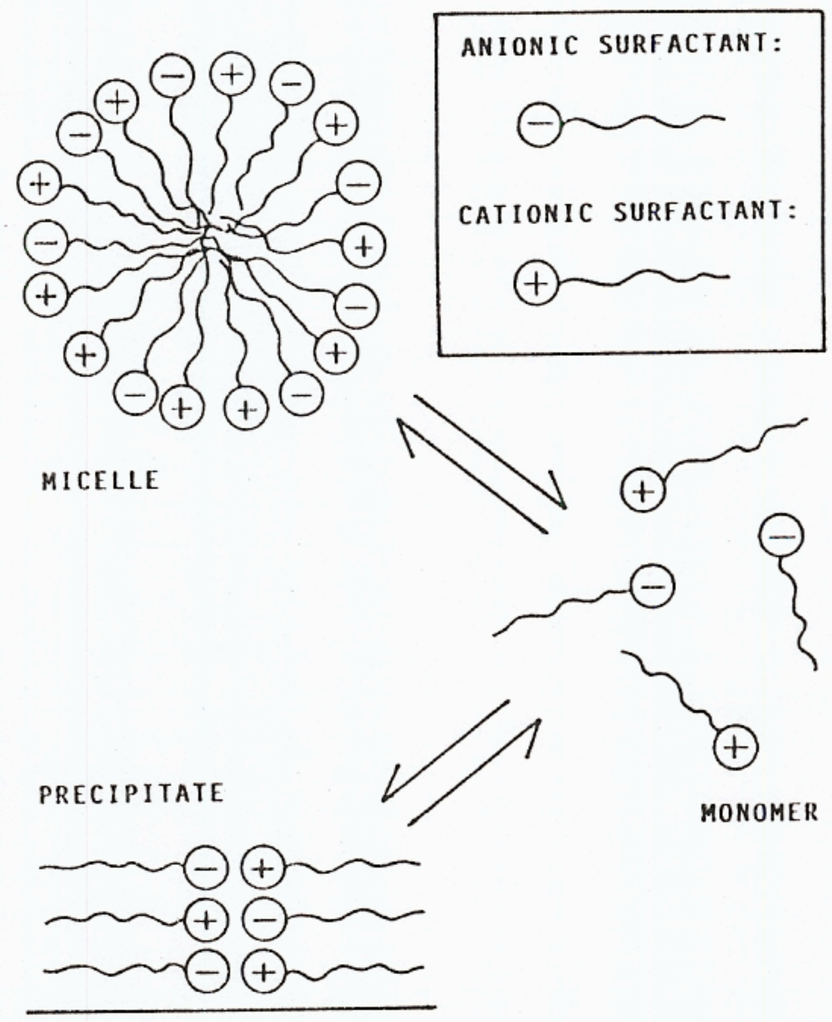

FIG. 1. Schematic diagram of basic equilibria in system.

surface or present as unassociated ions in solution.

The formation of precipitate can be represented by

$$DS^- (aq) + DP^+ (aq) \rightleftharpoons DSDP (s),$$

where DSDP represents the salt that is formed from a 1:1 reaction between dodecyl sulfate anion (DS^-) and dodecylpyridinium cation (DP^+) in solution. This reaction can be described by a simple solubility product between the ions,

$$K_{sp} = [DS^-]_{mon}[DP^+]_{mon} f_{\pm}^2, \qquad [1]$$

where K_{sp} is the solubility product, $[DS^-]_{mon}$ and $[DP^+]_{mon}$ are the anionic and cationic surfactant monomer concentrations, respectively, and $f_\pm$ is the activity coefficient in solution. The extended Debye–Huckel equation proposed by Davies (30) is used to estimate $f_\pm$,

$$\log f_\pm = -0.5139|z_+ z_-| \times \{\sqrt{I}/(1 + \sqrt{I}) - 0.3I\}, \qquad [2]$$

where I is the ionic strength.

The purpose of the model is to calculate where the precipitation phase boundaries are located, i.e., at which concentrations only an infinitesimal amount of precipitate is present in solution. On the boundary, therefore, all surfactant can be assumed to be present in mixed micelles or as monomer. An overall material balance on each surfactant yields

$$C_{NaDS} = [DS^-]_{mon} + [DS^-]_{mic} \quad [3]$$

$$C_{DPCl} = [DP^+]_{mon} + [DP^+]_{mic}, \quad [4]$$

where C_{NaDS} and C_{DPCl} represent the total concentration of NaDS and DPCl in solution, respectively, and the concentration of each surfactant in mixed micelles is given by $[DS^-]_{mic}$ and $[DP^+]_{mic}$.

In order to calculate the monomer concentration of each surfactant, it is necessary to model the monomer–micelle equilibrium. In general, the composition in the monomer will be different than the micellar composition (surfactant-only basis). Regular solution theory has been widely used to model this equilibrium in surfactant mixtures (24, 31–35) and will also be used here. By assuming the micelles are a surfactant pseudo-phase and applying regular solution theory,

$$[DS^-]_{mon} = X_{DS}CMC_{DS}\exp\{(1 - X_{DS})^2 W/RT\} \quad [5]$$

$$[DP^+]_{mon} = (1 - X_{DS})CMC_{DP}\exp\{(X_{DS})^2 W/RT\}, \quad [6]$$

where CMC_{DS} and CMC_{DP} are the CMC values of the pure surfactants, NaDS and DPCl, at the same electrolyte concentration as the mixed surfactant system of interest, W is the interaction parameter, R is the ideal gas constant, and T is the absolute temperature. The mole fraction of surfactant in the micelles, X_{DS} (and $X_{DP} = 1 - X_{DS}$), is on a surfactant-only basis so that

$$X_{DS} = [DS^-]_{mic}/\{[DS^-]_{mic} + [DP^+]_{mic}\}. \quad [7]$$

All samples in this study have 0.15 M added NaCl which is assumed to be swamping electrolyte; i.e., counterions (Na^+ and Cl^-) added to solution from the surfactants are negligible compared to the added NaCl. This simplifies the model in that CMC_{DS} and CMC_{DP} can be assumed constant for all solutions. In addition, the fraction of the total counterions bound onto the charged micelles is considered insignificant due to swamping NaCl. Ionic strength calculations, however, do include surfactant concentrations so

$$I = 0.15 + C_{NaDS} + C_{DPCl}, \quad [8]$$

where I is in molarity.

In general, it may not be possible to use the simplifications allowed by swamping electrolyte, for instance when no NaCl is added. In such systems it would be necessary to model CMC_{DS} and CMC_{DP} as a function of unbound electrolyte (24, 34) which would also require an understanding of counterion binding on the mixed anionic–cationic micelles (36, 37).

When phase boundaries are determined experimentally, the total concentration of one of the surfactants is an independent variable. So, if C_{NaDS} is set, the dependent variable of interest is the total concentration of DPCl required to cause precipitation. If K_{sp}, W/RT, CMC_{DS}, and CMC_{DP} are known, Equations [1]–[8] can be solved simultaneously for C_{DPCl}, $[DS^-]_{mon}$, $[DP^+]_{mon}$, $f_\pm$, I, X_{DS}, $[DS^-]_{mic}$, and $[DP^+]_{mic}$. Therefore, the model developed here can be used to predict the precipitation phase boundary.

RESULTS AND DISCUSSION

Composition of Precipitate

Elemental analysis of the precipitate formed between NaDS and DPCl in solution is given in Table I. The S/N mole ratio was determined to be 1.0 which confirms a reaction stoichiometry of 1:1; however, it is puzzling that 0.86% Na was found in the precipitate. The Na here is probably not from NaCl left on the crystals because Cl is virtually absent. At the same time, it does not seem likely that coprecipitation of NaDS is occurring because this would increase the S/N mole ratio. Several

TABLE I

Analysis of Precipitate Formed between NaDS and DPCl in Solution

Element	Calculated[a]	Found
C	67.85	67.81
H	10.71	10.78
O	12.47	12.23
N	2.73	2.72
N (dup.)		2.64
S	6.24	6.08
S (dup.)		6.25
Na	None	0.86
Cl	None	0.11

[a] Weight percent based on 1:1 complex.

other workers have determined the compositions of similar systems and also concluded a 1:1 complex was formed (17, 38, 39).

Precipitation without Micelles Present

At low surfactant concentrations, where micelles are not present, it is possible to determine the solubility product, K_{sp}, from precipitation data. Under these conditions the monomer concentrations in Eq. [1] are equal to the respective total concentrations of each surfactant. One can further manipulate Eq. [1] to obtain

$$\log C_{DPCl} = -\log C_{NaDS} + \log(K_{sp}/f_{\pm}^2). \quad [9]$$

In this region, surfactant concentrations are so low they essentially do not affect ionic strength, because of swamping NaCl, so $f_{\pm}$ can be considered to have a constant value (0.758). Therefore, from Eq. [9], precipitation data should give a straight line with a slope of -1 and from the intercept it is possible to calculate K_{sp}. Experimental results are given in Fig. 2 where K_{sp} is calculated to be $2.24 \times 10^{-10}\ M^2$.

From Fig. 2 it is evident that at these very low surfactant concentrations it is not easy to detect the actual location of the precipitation boundary. Visual determination is limited because it is very difficult to see less than 3×10^{-6} M formed precipitate. Analytical instruments such as a surfactant selective electrode or UV spectrophotometer are limited because they cannot detect surfactant concentrations below approximately 5×10^{-6} M. Surface tension measurements and laser scattering experiments proved to be the most useful techniques to determine onset of precipitation when visual determination was limited. Although surface tension is usually used to determine formation of micelles (CMC), it can also be used to detect precipitate or coacervate formation (2, 40). Figure 3 shows surface tension as a function of total surfactant concentration in a NaDS–DPCl mixture when the mole fraction of NaDS is held constant at 0.990 (surfactant-only basis). The concentration at the break in this curve corresponds to a point on the phase boundary shown in Fig. 2.

It seems appropriate at this point to mention another reaction that can occur in mixtures of large organic ions with opposite charges: ion pair formation. This can be represented by

$$K_{ip} = [DS^-DP^+]/\{[DS^-]_{mon}[DP^+]_{mon}\}, \quad [10]$$

where K_{ip} is the ion pair constant and DS^-DP^+ represents the soluble ion pair which is considered to be a charged entity (unlike precip-

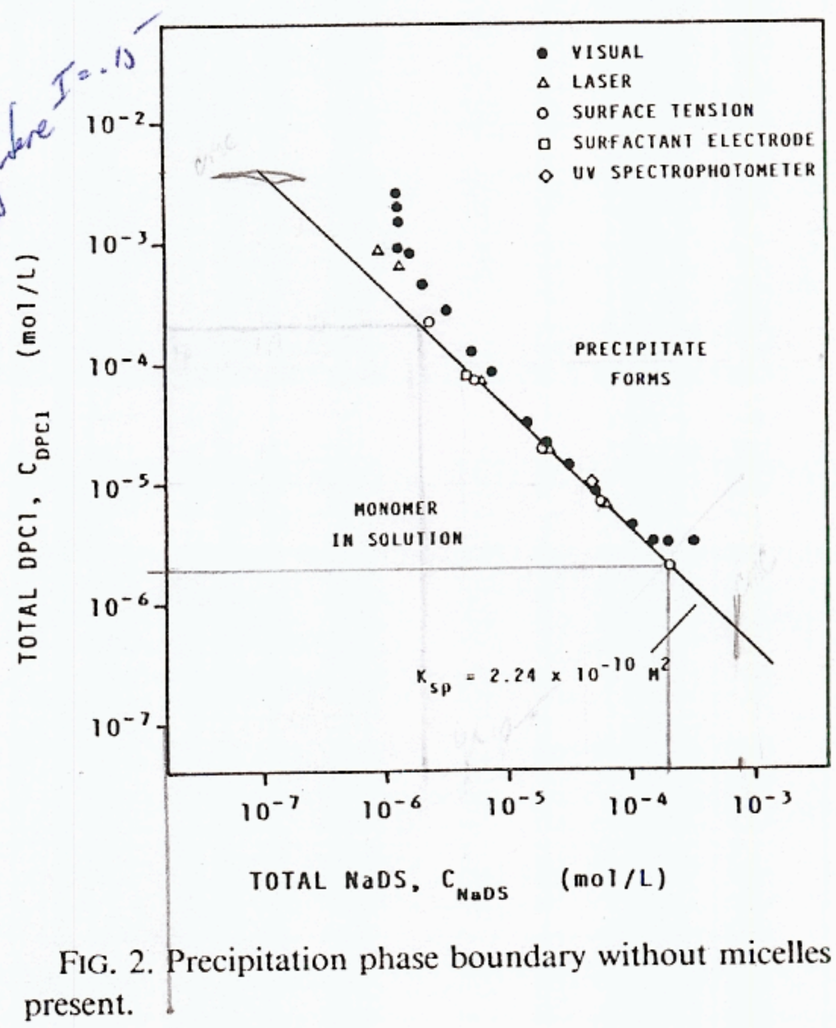

FIG. 2. Precipitation phase boundary without micelles present.

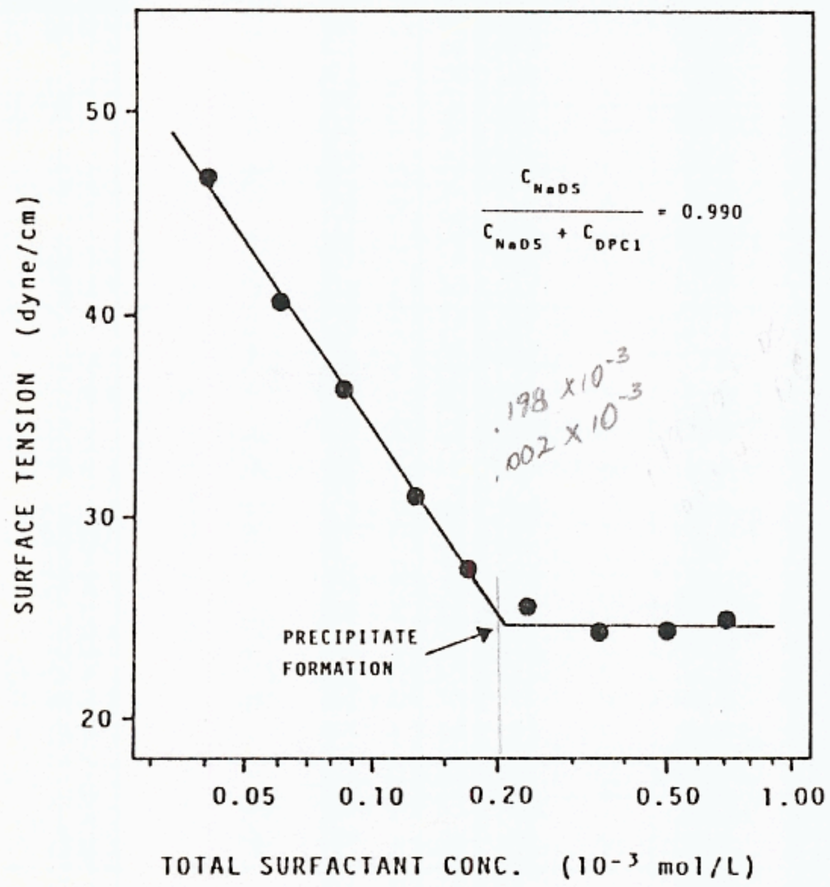

FIG. 3. Detection of precipitate formation using surface tension measurements.

itate) held together by both hydrophobic and electrostatic interactions. Tomlinson (1) has presented ion pair association constants for several systems and a value of 9.61×10^6 (mole fraction basis) can be obtained from data reported by Mitsuishi (41) on the NaDS–DPCl system. Using this number, and by combining Eqs. [1] and [10], the ion pair concentration, $[DS^-DP^+]$, is calculated to be 4.0×10^{-6} M and should be constant along the entire phase boundary. This value seems too large considering that if this much ion pairing occurred in these solutions, the precipitation boundary would not extend below 4.0×10^{-6} M for either surfactant. However, from Fig. 2, the phase boundary is linear to about 2×10^{-6} M and precipitate can be detected down to 1×10^{-6} M NaDS. Therefore, in this study, ion pair formation will be neglected. There is no doubt that ion pairing can take place; however, it is probably more important in dye–surfactant systems of opposite charge where pseudomicelles can form.

Supersaturation is also a very important consideration in determining the concentration at which precipitate begins to form (42). In surfactant systems with inorganic counterions, it has been clearly shown that precipitation boundaries change as a function of time (22). In mixed surfactant and surfactant–dye systems, observations confirm that solutions can remain clear for long periods of time, even days, before precipitate begins to form (2, 17, 26, 38). This problem can be avoided if samples are cooled so that precipitate is forced to form (as discussed under Experimental) and then solutions are allowed to equilibrate at the temperature of interest. Much of the precipitation and ion pairing work that has been done has neglected to deal with the problem of supersaturation.

Precipitation with Micelles Present

The CMCs for the pure surfactants with 0.15 M added NaCl were measured: $CMC_{DS} = 7.7 \times 10^{-4}$ M and $CMC_{DP} = 4.0 \times 10^{-3}$ M. Using the value of K_{sp} determined in Fig. 2 and with $W/RT = -8.62$ (which will be discussed later), Eqs. [1]–[8] were solved simultaneously to give the calculated precipitation boundaries with micelles in solution. The results are shown in Fig. 4.

From Fig. 4 it is evident that as the monomer–precipitate line approaches the CMC of either pure surfactant, drastic changes occur in the solutions. These sharp breaks along the phase boundary correspond to the points where micelles begin to form in solution. From these points, the precipitation boundary extends as two branches; one branch is DPCl-rich and the other is NaDS-rich. Along the DPCl-rich branch of the phase boundary, calculations from the model are very close to the experimental data. However, the calculated precipitation boundary for the NaDS-rich branch shows substantial deviation from experimental measurements, which is no doubt related to coacervate formation.

Coacervation refers to the formation of small droplets in solution which are rich in surfactant. These coalesce over a period of time so that the original solution separates into two isotropic liquids: one is rich in surfactant and therefore usually viscous, and the other

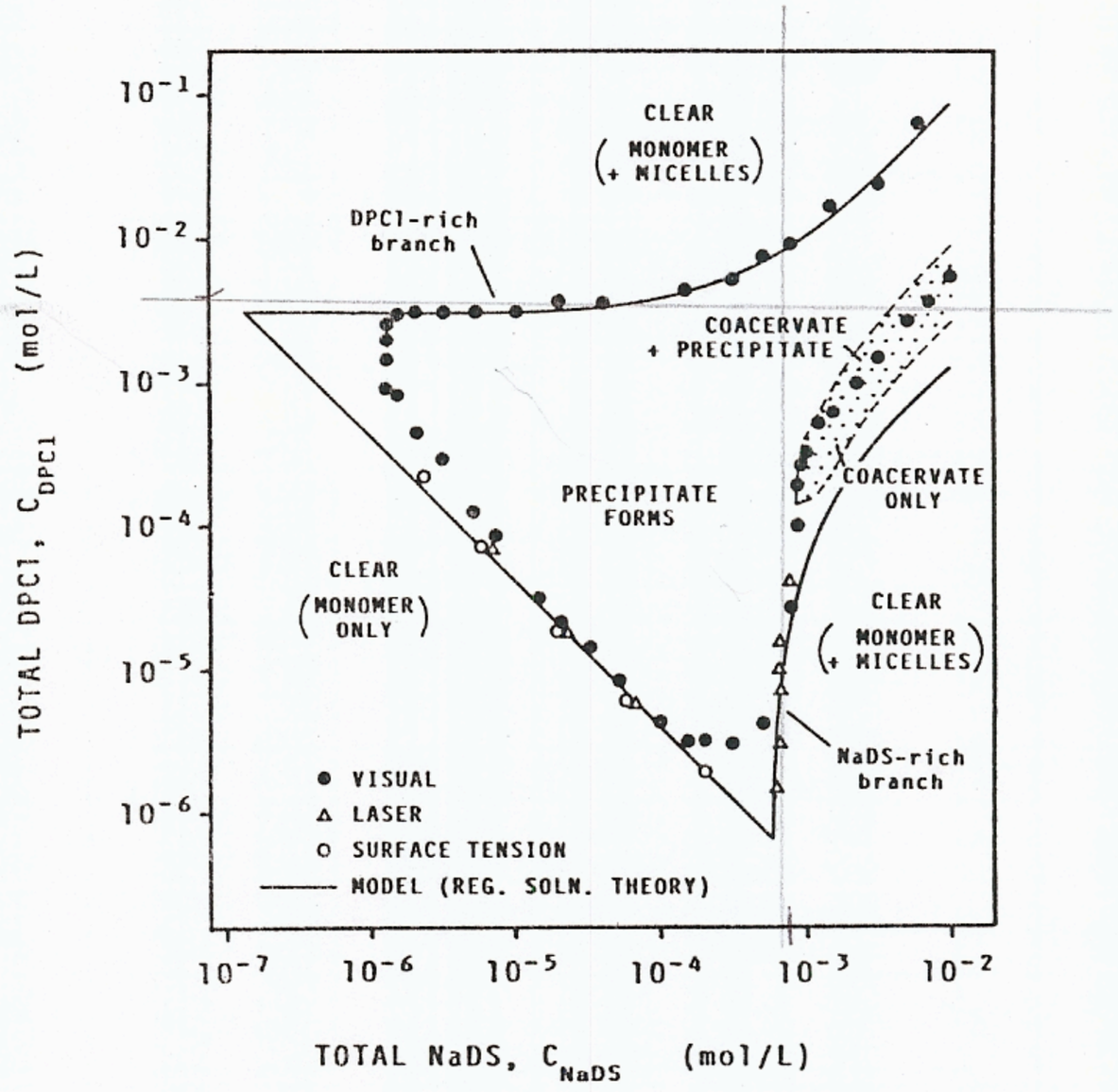

FIG. 4. Complete precipitation phase boundary with predictions using regular solution theory.

contains little surfactant. Figure 4 shows that in some of the solutions studied here only coacervate forms, while in other solutions both coacervate and precipitate form; i.e., the precipitation boundary lies within the region where coacervate may form. Indeed, in some solutions it is difficult to determine the presence of precipitate due to turbidity caused by coacervate that has not settled out of solution. In addition, there is a narrow range of solution concentrations, close to the precipitation boundary and within the coacervate region, where there seems to be a transition from viscous coacervate to oily precipitate to crystalline precipitate.

Coacervation has been thoroughly investigated in systems similar to the one studied here and it is generally believed to be caused by the growth of micelles to very large sizes (2, 43–46). Interestingly, in a study of micelle aggregation numbers for a mixture of NaDS and dodecyltrimethylammonium chloride (DTAC), the DTAC-rich micelles showed only a moderate increase in size as the precipitation boundary was approached, whereas the NaDS-rich micelles showed a dramatic size increase (47). This is consistent with the results in Fig. 4 where coacervation only occurs along the NaDS-rich branch.

Although coacervation is a very important topic in interactions between large organic ions of opposite charge (1), the focus of the work here will be on precipitation. In order to gain more understanding about the precipitation phase boundary and why it has two branches extending from the monomer–precipitate line, Eqs. [1], [5], and [6] are combined to give

$$K_{sp}/f_{\pm}^2 = (X_{DS} - X_{DS}^2)CMC_{DS}CMC_{DP} \times \exp\{[1 - 2(X_{DS} - X_{DS}^2)]W/RT\}. \quad [11]$$

Since $f_{\pm}$ is practically constant, and all other parameters are constant, only one value of $(X_{DS} - X_{DS}^2)$ will satisfy Eq. [11]. This means there are two values of X_{DS} (one DPCl-rich and one NaDS-rich) that occur on the precipitation

phase boundary where micelles are present and furthermore, if $f_{\pm}^2$ is essentially constant, these values of X_{DS} are constant along each branch. This can be explained in more detail by considering monomer–micelle equilibrium.

The CMC for a mixed surfactant system can be considered as a type of phase boundary between monomer and micelles with specific compositions. Figure 5 shows this boundary for micelle formation along with the monomer–precipitate boundary calculated from Fig. 2. Points A and B in Fig. 5 show where the monomer–micelle boundary intersects the monomer–precipitate boundary. These points represent where monomer, micelles, and precipitate are in equilibrium. Point C represents a solution on the monomer–micelle boundary that could never exist. Precipitate would form in a sample at this point so that equilibrium concentrations of surfactant remaining in solution will never exceed the monomer–precipitate line and no micelles would remain in solution. Point D represents a solution in which no precipitate will form because the monomer concentrations are below the precipitate line determined by K_{sp}. At concentrations slightly greater than point D, but still below the precipitation line, only monomer and micelles exist in solution. Therefore, for any solution to be on the precipitation phase boundary and contain micelles, it must have the monomer concentrations existing at points A or B and a corresponding micelle mole fraction given by monomer–micelle equilibrium.

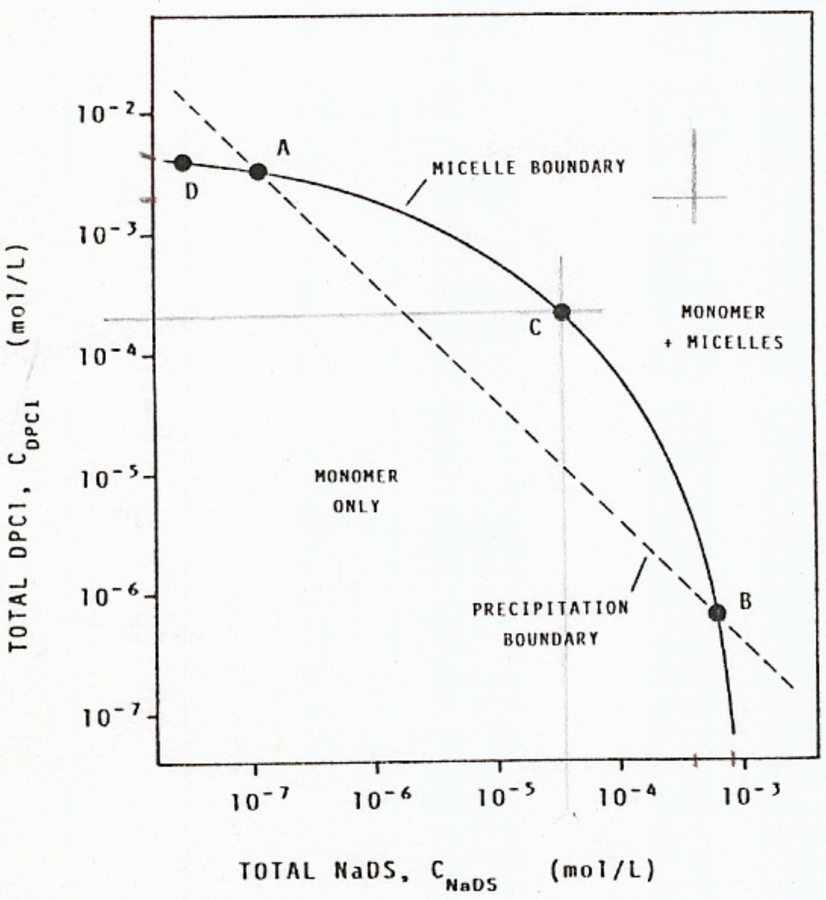

FIG. 5. Monomer–micelle and monomer–precipitate phase boundaries.

For example, at point A the monomer concentrations of each surfactant are equal to the total concentrations since it is on the phase boundary. Therefore, $C_{DPCl} = [DP^+]_{mon} = 3.0 \times 10^{-3}$ M and $C_{NaDS} = [DS^-]_{mon} = 1.3 \times 10^{-7}$ M, which gives a monomer mole fraction (surfactant-only basis) of 4.3×10^{-5} for NaDS at point A. Equation [11] can be solved to show that the corresponding mole fraction in the micelle is $X_{DS} = 0.124$ at this point. These mole fractions are constant along the entire DPCl-rich branch of the precipitation phase boundary in Fig. 4 (assuming that the change in ionic strength is negligible).

If C_{DPCl} is increased by 4.5×10^{-4} M above point A, then to remain on the precipitation phase boundary, C_{NaDS} must be increased 6.4×10^{-5} M (so $X_{DS} = 0.124$) and all added surfactant forms micelles because the monomer concentrations must remain constant. An increase from 3.0×10^{-3} to 3.45×10^{-3} M is a small change for the total DPCl concentration as seen in Fig. 4, but an increase from 1.3×10^{-7} to 6.4×10^{-5} M is a tremendous jump in the total NaDS concentration. Of course, a similar argument can be made for the NaDS-rich branch of the phase boundary beginning at point B. This accounts for why drastic changes are seen at the two points on the phase boundary when micelles begin to form.

If total DPCl concentration is increased above the DPCl-rich branch of the phase boundary, and C_{NaDS} is held constant, precipitate cannot form. This is due to a change in micelle composition, from added DPCl, which in turn affects the monomer composition. The monomer concentrations are now below the monomer–precipitate line (represented by point D in Fig. 5) so that precipitate cannot form at these surfactant concentrations. In

C_φ 2.00×10^{-4}

C_L 3.55×10^{-5}

because there are only two monomer compositions where monomer, micelles, and precipitate are in equilibrium; so, from regular solution theory, there are two corresponding values of X_{DS}. However, in the vicinity of the calculated NaDS-rich branch, where the model fails, monomer–micelle equilibrium is affected by micelles growing in size and eventual coacervate formation at higher DPCl concentrations. When DPCl concentration is increased until precipitate begins to form, it represents the point where monomer concentrations intersect the monomer–precipitate line (as discussed from Fig. 5). For this specific monomer composition, there is a corresponding micelle composition and coacervate composition (when present), which should be constant along the entire precipitation boundary. Therefore, the mole fraction of DS^- that is aggregated as micelles and coacervate, X^*_{DS}, can be represented by

$$X^*_{DS} = [DS^-]_{agg}/\{[DS^-]_{agg} + [DP^+]_{agg}\}, \quad [12]$$

where $[DS^-]_{agg}$ and $[DP^+]_{agg}$ represent the concentrations of each surfactant that are aggregated, either as micelles or coacervate. In this work, X^*_{DS} is assumed to be constant although, strictly speaking, it is only a constant when (i) the amount of surfactant present in micelles is insignificant compared to the concentration of surfactant in coacervate, and/or (ii) the composition in the micelles is approximately the same as the coacervate composition.

It is possible to determine the value of X^*_{DS} for each branch of the precipitation boundary using the experimental data in Fig. 4. At high concentrations essentially all of the surfactant is present as micelles or coacervate; i.e., the monomer concentrations are negligible so $[DS^-]_{agg} = C_{NaDS}$ and $[DP^+]_{agg} = C_{DPCl}$. Using this fact, with Eq. [12] and data in Fig. 4, X^*_{DS} is calculated to be 0.107 for the DPCl-rich branch. This is very close to the value of X_{DS} that was calculated using regular solution theory, which is not surprising because Eq. [12] reduces to Eq. [7] when coacervate is not present. From data for the NaDS-rich branch, X^*_{DS} is found to be 0.620 which compares to 0.876 calculated using regular solution theory.

To be consistent, the material balances (Eqs. [3] and [4]) should now be written as

$$C_{NaDS} = [DS^-]_{mon} + [DS^-]_{agg} \quad [13]$$

$$C_{DPCl} = [DP^+]_{mon} + [DP^+]_{agg}. \quad [14]$$

By combining Eqs. [13] and [14] with Eq. [12], upon rearrangement it can be shown that

$$C_{DPCl} = [DP^+]_{mon} + (1 - X^*_{DS})(C_{NaDS} - [DS^-]_{mon})/X^*_{DS}. \quad [15]$$

This equation, therefore, can model both branches of the precipitation boundary when the appropriate values for X^*_{DS}, $[DS^-]_{mon}$, and $[DP^+]_{mon}$ are used for each branch. The results are shown in Fig. 6.

It should be stressed that monomer concentrations used in Eq. [15] are taken to be the points where each branch intersects the monomer–precipitate line (points A and B in Fig. 5, as discussed earlier). This assumes, however, that monomer concentrations are constant along each branch of the boundary, which may not necessarily be true for the NaDS-rich branch due to micellar growth and coacervation. This is not an important consideration, though, because any error in $[DS^-]_{mon}$ is insignificant compared to C_{NaDS} which is usually a much larger number. Figure 6 shows that Eq. [15] fits the data well for each branch of the precipitation boundary (Eq. [9] is still used for the monomer–precipitate line). It is interesting to note that the phase boundary between coacervate formation and clear solution, in Fig. 6, can be described very well when a value of 0.773 is used for X^*_{DS}. Dubin and Davis (53) describes a similar result for a surfactant–polymer system where coacervation occurred only within a certain range of mole fractions.

Prediction of Total Precipitate Formed

With the entire precipitation boundary successfully modeled, it is possible to calculate how much precipitate will form in any mixture

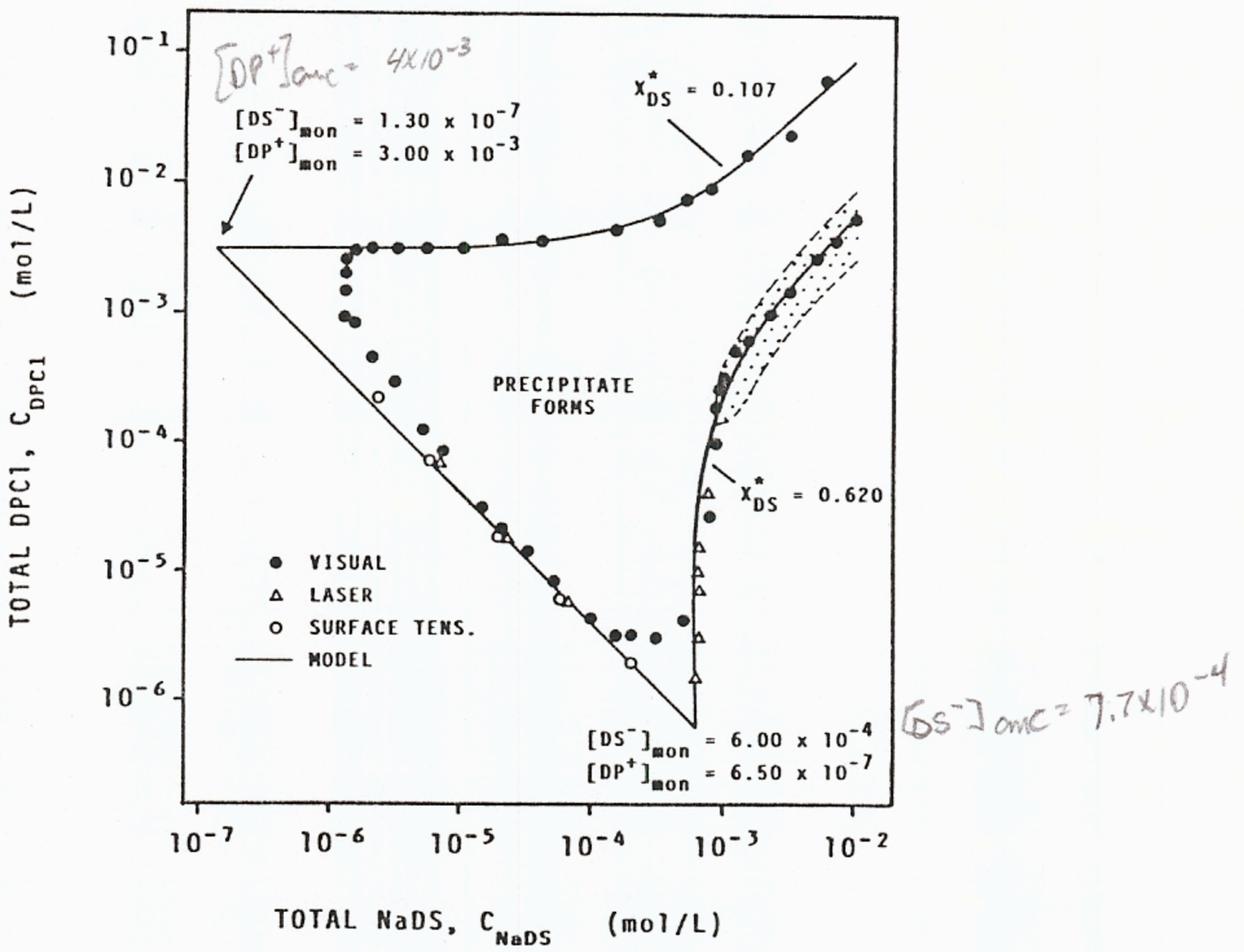

FIG. 6. Comparison between precipitation data and calculations from empirical model.

of NaDS and DPCl in solution. The concentration of each surfactant remaining in a solution after precipitation will be given by the equilibrium location on the phase boundary. To calculate the path by which a solution reaches the phase boundary, one can write equations that apply at any time during precipitation,

$$C_{NaDS} = [DS^-]_{unr} + [DS^-]_{ppt} \quad [16]$$

$$C_{DPCl} = [DP^+]_{unr} + [DP^+]_{ppt}, \quad [17]$$

where $[DS^-]_{unr}$ and $[DP^+]_{unr}$ represent the concentration of each surfactant that is unreacted, and, $[DS^-]_{ppt}$ and $[DP^+]_{ppt}$ are the concentrations of each surfactant that have reacted to form precipitate. Furthermore

$$[DS^-]_{ppt} = [DP^+]_{ppt} = [DSDP] \quad [18]$$

because the reaction stoichiometry has been shown to be 1:1 (DS^-:DP^+). Combining Eqs. [16]–[18] gives

$$C_{NaDS} - C_{DPCl} = [DS^-]_{unr} - [DP^+]_{unr} = D, \quad [19]$$

where D is the concentration difference between unreacted surfactants which will be a constant along the entire precipitation pathway. Figure 7 shows curves of constant D superimposed on the precipitation phase boundary. Therefore, for any mixture of NaDS and DPCl inside the precipitation region, as precipitate forms, the solution concentrations will change along a curve of constant D as shown in Fig. 7 and equilibrium concentrations of surfactant remaining in solution (after precipitation is complete) are given by the point of intersection between the appropriate concentration difference curve and the phase boundary. These type of curves have also been used in precipitation of anionic surfactants with inorganic cations (21, 54).

It is possible to explicitly calculate the amount of precipitate that forms by expanding

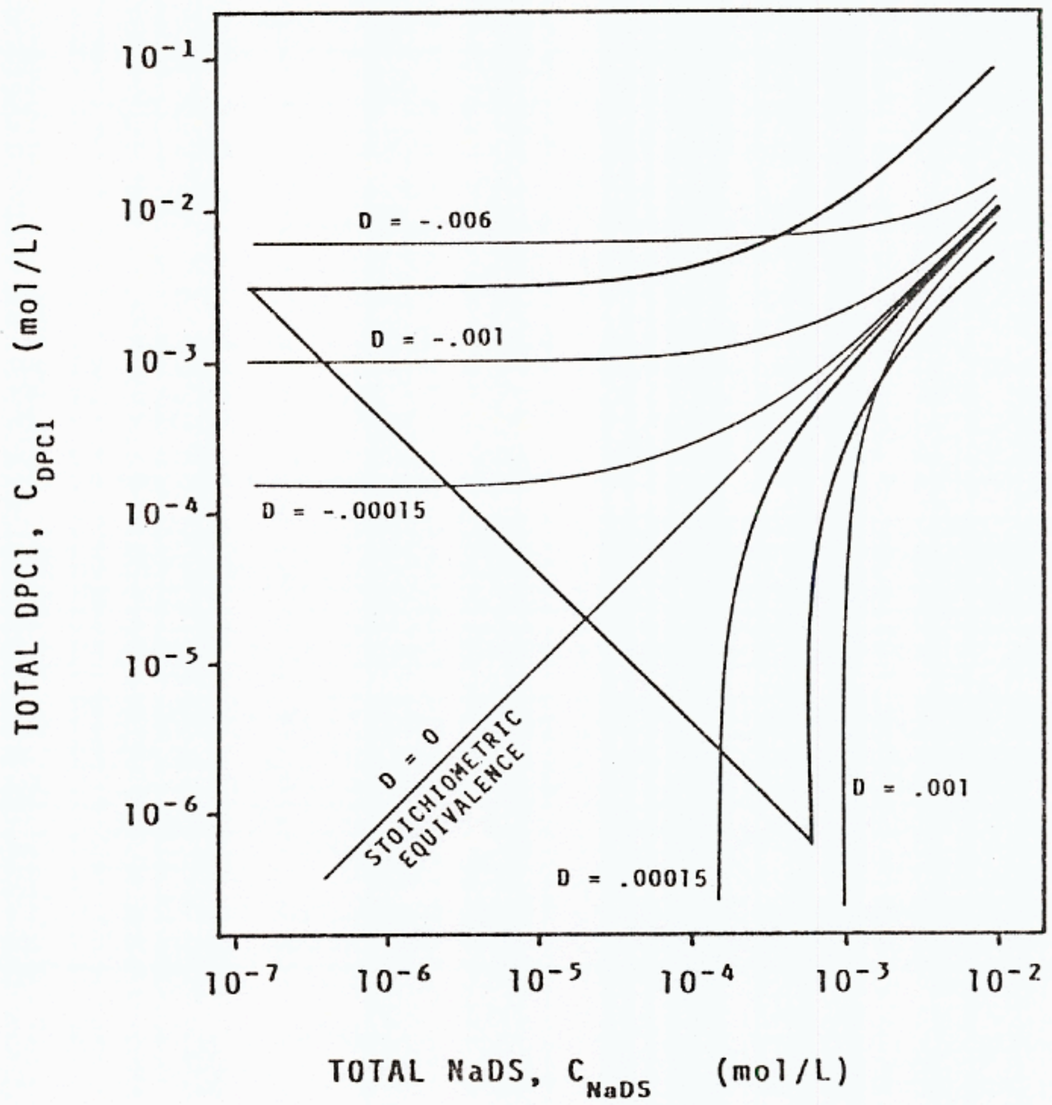

FIG. 7. Paths of precipitate formation in relation to the equilibrium precipitation boundary.

material balance Eqs. [13] and [14] to include precipitate:

$$C_{NaDS} = [DS^-]_{mon} + [DS^-]_{agg} + [DSDP] \quad [20]$$

$$C_{DPCl} = [DP^+]_{mon} + [DP^+]_{agg} + [DSDP]. \quad [21]$$

These are substituted into Eq. [12] to yield

$$[DSDP] = \{X^*_{DS}(C_{DPCl} - [DP^+]_{mon}) + (X^*_{DS} - 1)(C_{NaDS} - [DS^-]_{mon})\}/(2X^*_{DS} - 1), \quad [22]$$

which is only valid if there are micelles present after precipitation; i.e., the precipitation pathway intersects either the NaDS-rich or DPCl-rich branch of the phase boundary. If there are no micelles after precipitation then the concentrations of aggregated surfactant in Eqs. [20] and [21] are zero. These are combined with Eq. [1] to give

$$K_{sp}/f^2_{\pm} = (C_{NaDS} - [DSDP]) \times (C_{DPCl} - [DSDP]). \quad [23]$$

Therefore, if $C_{NaDS} - C_{DPCl} = D > 6.0 \times 10^{-4}$ M then Eq. [22] can be solved to determine [DSDP] using $X^*_{DS} = 0.620$, $[DS^-]_{mon} = 6.0 \times 10^{-4}$ M, and $[DP^+]_{mon} = 6.5 \times 10^{-7}$ M. Equation [22] is also used when $D < -3.0 \times 10^{-3}$ M where $X^*_{DS} = 0.107$, $[DS^-]_{mon} = 1.3 \times 10^{-7}$ M, and $[DP^+]_{mon} = 3.0 \times 10^{-3}$ M. At all values of D between these, Eq. [23] can be used to calculate the amount of precipitate that forms.

Predictions from Eqs. [22] and [23] for several NaDS–DPCl mixtures are summarized in Table II and experimental results are shown in Fig. 8. To determine [DSDP] experimentally, solutions were centrifuged after precipitation and allowed to reequilibrate at 30°C. Supernatant was removed and diluted to below the monomer–precipitate line and concentrations of DP^+ were determined using a

TABLE II

Comparison between Predicted and Measured Amounts of DSDP Precipitated

Total concentration in solution[a]		Measured concentrations after precipitation		Predicted from model	Path shown
C_{DPCl}	C_{NaDS}	$[DP^+]_{mon} + [DP^+]_{agg}$	[DSDP]	[DSDP]	in fig. 8
0.800	1.000	0.004	0.796	0.798	E–E*
1.000	1.000	0.011	0.989	0.980	F–F*
2.000	1.000	0.944	1.056	1.000	G–G*
6.000	5.000	0.744	5.256	5.000	H–H*
4.000	5.000	0.945	3.055	3.367	I–I*
10.000	4.000	6.250	3.750	3.592	J–J*
1.400	1.000	0.331	1.069	0.999	K–K*

[a] All concentrations in 10^{-3} moles/liter.

UV spectrophotometer and standard solutions. The amount of precipitate that forms can be obtained from the difference between C_{DPCl} and the measured equilibrium concentration of DP^+ (after precipitation). Table II shows there is good agreement between predicted and measured [DSDP] values.

CONCLUSIONS

Mixtures of NaDS and DPCl react in solution to form precipitate over a wide range of concentrations. When no micelles are present in solution, this reaction can be modeled by a simple solubility product between the to-

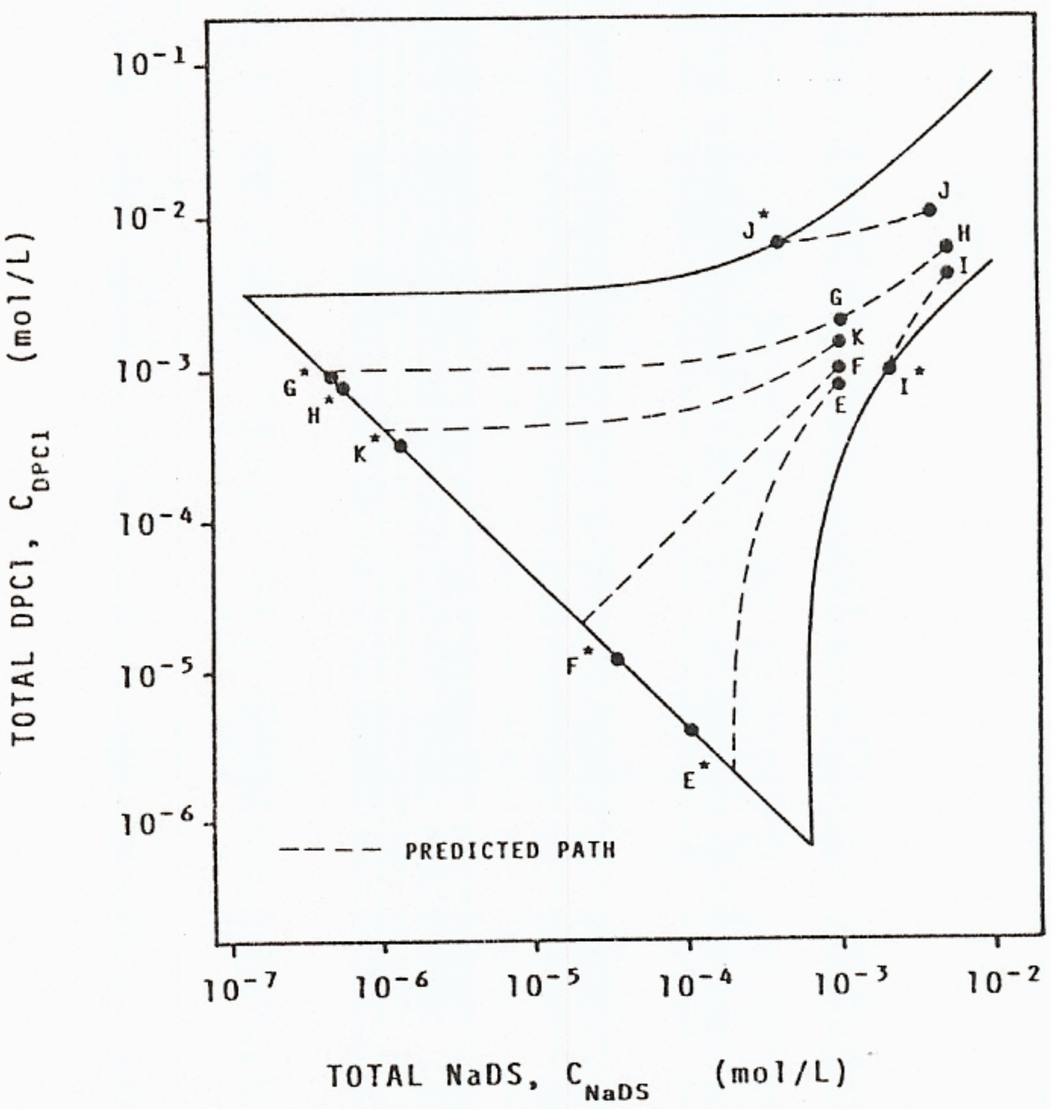

FIG. 8. Comparison between predicted and measured equilibrium concentrations for several NaDS–DPCl mixtures.

tal surfactant concentrations. When micelles are present, monomer concentrations are used in the solubility product expression and the monomer–micelle equilibrium can be described using regular solution theory. From this approach, it can be shown that there are only two monomer compositions (one NaDS-rich and one DPCl-rich) where monomer, micelles, and precipitate can exist in equilibrium. Furthermore, these monomer compositions and the corresponding micelle compositions are constant along each branch of the precipitation phase boundary. The model that is developed predicts precipitation data quite well except in the case where coacervate also forms in solution.

To predict precipitation boundaries when coacervate is present, an empirical model is developed. In this case, the monomer composition where precipitation occurs corresponds to specific micelle and coacervate compositions which are assumed to remain constant along the precipitation boundary. Using this fact, combined with a material balance for each surfactant, an equation is developed which calculates precipitation boundaries with or without coacervate present. In addition, a simple extension of this approach provides an explicit equation which predicts the amount of precipitate that forms in any NaDS–DPCl mixture so that the equilibrium surfactant concentrations (after precipitation) can also be determined.

It is hoped that this work can be extended to other mixtures of large organic ions with opposite charge such as surfactant–dye and surfactant–polymer systems. This would require a thorough understanding of surfactant-poor regions where micellization does not occur over a narrow concentration range, if at all. Supersaturation may also prove to be a very important consideration in obtaining phase boundary data for all of these systems but it has not yet been thoroughly investigated.

ACKNOWLEDGMENTS

Financial support for this work was provided by the Mobil Research and Development Corp., the Shell Development Co., Arco Oil and Gas Co., DOE Contract No. DE-AC19-85BC10845, the OU Energy Resources Institute, and the Oklahoma Mining and Minerals Resources Research Institute.

REFERENCES

1. Tomlinson, E., Davis, S. S., and Mukhayer, G. I., *in* "Solution Chemistry of Surfactants" (K. L. Mittal, Ed.), Vol. 1, p. 3. Plenum, New York, 1979.
2. Barry, B. W., and Russel, G. F. J., *J. Pharm. Sci.* **61,** 502 (1972).
3. Attwood, D., and Florence, A. T., "Surfactant Systems," p. 388. Chapman & Hall, New York, 1983.
4. Tomlinson, E., and Davis, S. S., *J. Colloid Interface Sci.* **66,** 335 (1978).
5. Diaz Garcia, M. E., and Sanz-Medel, A., *Talanta* **33,** 255 (1986).
6. Mukerjee, P., and Mysels, K. J., *J. Amer. Chem. Soc.* **77,** 2937 (1955).
7. Nagarajan, R., and Harold, M. P., *in* "Solution Behavior of Surfactants" (K. L. Mittal, Ed.), Vol. 2, p. 1391, Plenum, New York, 1980.
8. Sabbadin, J., Le Moigne, J., and Francois, J., *in* "Surfactants in Solution" (K. L. Mittal, Ed.), Vol. 2, p. 1377. Plenum, New York, 1984.
9. Shah, D. O., and Walker, R. D., "Research on Surfactant–Polymer Oil Recovery Systems," University of Florida, 1980 Annual Report for U.S. DOE Contract No. DE-AC1979BC10075.
10. Great Britain Patent 2,122,898 (1984) [*Chem. Abstr.* **101,** 12011w].
11. Japan Patent 59,187,095 (1984) [*Chem. Abstr.* **102,** 190833u].
12. Japan Patent 60,115,511 (1985) [*Chem. Abstr.* **103,** 220601g].
13. Sadhukhan, B. K., and Chattoraj, D. K., *in* "Surfactants in Solution" (K. L. Mittal, Ed.), Vol. 2, p. 1249. Plenum, New York, 1984.
14. Zheng, Y., Longdi, L., and Sun, S., *Huaxue Tongbao* **18,** 16 (1983) [*Chem. Abstr.* **100,** 131587c].
15. Birch, B. J., and Cockroft, R. N., *Ion-Sel. Electrode Rev.* **3,** 1 (1981).
16. Lin, W., Tang, M., Stranahan, J. J., and Deming, S. N., *Anal. Chem.* **55,** 1872 (1983).
17. Scowen, R. V., and Leja, J., *Canad. J. Chem.* **45,** 2821 (1967).
18. USSR Patent 1,028,605 (1983) [*Chem. Abstr.* **100,** 12144w].
19. Schwuger, M. J., *Kolloid Z.* **243,** 129 (1971).
20. Kallay, N., Pastuovic, M., and Matijevic, E., *J. Colloid Interface Sci.* **106,** 452 (1985).
21. Matheson, K. L., Cox, M. F., and Smith, D. L., *J. Amer. Oil Chem. Soc.* **62,** 1391 (1985).
22. Peacock, J. M., and Matijevic, E., *J. Colloid Interface Sci.* **77,** 548 (1980).
23. Celik, M. S., Manev, E. D., and Somasundaran, P., *AIChE Symp. Ser.* **78,** 86 (1982).

24. Stellner, K. L., and Scamehorn, J. F., *J. Amer. Oil Chem. Soc.* **63,** 566 (1986).
25. Stellner, K. L., and Scamehorn, J. F., "Improving Hardness Tolerance of Anionic Surfactant Solutions by Addition of Nonionic Surfactants," 77th National American Oil Chemist's Society Meeting, Honolulu, May, 1986.
26. Reeves, R. L., and Harkaway, S. A., *in* "Micellization, Solubilization, and Microemulsions" (K. L. Mittal, Ed.), Vol. 2, p. 819. Plenum, New York, 1977.
27. Burdett, B. C., *in* "Aggregation Processes in Solution" (E. Wyn-Jones and J. Gormally, Eds.), p. 241. Elsevier Science, New York, 1983.
28. Smith, D. L., Matheson, K. L., and Cox, M. F., *J. Amer. Oil Chem. Soc.* **62,** 1399 (1985).
29. Lunkenheimer, K., and Wantke, K. D., *Colloid Polym. Sci.* **259,** 354 (1981).
30. Davies, C. W., "Ion Association," p. 41. Butterworths, London, 1962.
31. Rubingh, D. N., *in* "Solution Chemistry of Surfactants" (K. L. Mittal, Ed.), Vol. 1, p. 337. Plenum, New York, 1979.
32. Holland, P. M., and Rubingh, D. N., *J. Phys. Chem.* **87,** 1984 (1983).
33. Holland, P. M., *Adv. Colloid Interface Sci.* **26,** 111 (1986).
34. Scamehorn, J. F., *in* "Phenomena in Mixed Surfactant Systems" (J. F. Scamehorn, Ed.), Vol. 311, p. 1. ACS Symp. Ser., ACS, Washington, 1986.
35. Rosen, M. J., and Hua, X. Y., *J. Amer. Oil Chem. Soc.* **59,** 582 (1982).
36. Rathman, J. F., and Scamehorn, J. F., *J. Phys. Chem.* **88,** 5807 (1984).
37. Hall, D. G., and Price, T. J., *J. Chem. Soc. Faraday Trans.* **80,** 1193 (1984).
38. Hoyer, H. W., and Doerr, I. L., *J. Phys. Chem.* **68,** 3494 (1964).
39. Nakamura, A., and Muramatsu, M., *J. Colloid Interface Sci.* **62,** 165 (1977).
40. Goddard, E. D., and Hannan, R. B., *J. Colloid Interface Sci.* **55,** 73 (1976).
41. Mitsuishi, M., and Hashizume, M., *Bull. Chem. Soc. Japan* **46,** 1946 (1973).
42. Skoog, D. A., and West, D. M., "Fundamentals of Analytical Chemistry," 2nd ed., p. 164. Holt, Rhinehart, & Winston, New York, 1969.
43. Mukhayer, G. I., and Davis, S. S., *J. Colloid Interface Sci.* **66,** 110 (1978).
44. Goodman, J. F., and Walker, T., *in* "Colloid Science" (D. H. Everett, Ed.), Vol. 3, p. 230. The Chemical Society, London, 1979.
45. Barry, B. W., and Gray, G. M. T., *J. Colloid Interface Sci.* **52,** 327 (1975).
46. Barry, B. W., and Gray, G. M. T., *J. Pharm. Sci.* **63,** 548 (1974).
47. Malliaris, A., Binana-Limbele, W., and Zana, R., *J. Colloid Interface Sci.* **110,** 114 (1986).
48. Hall, D. G., and Huddleston, R. W., *Colloids Surf.* **13,** 209 (1985).
49. Yoesting, O. E., and Scamehorn, J. F., *Colloid Polym. Sci.* **264,** 148 (1986).
50. Osborne-Lee, I. W., Schechter, R. S., and Wade, W. H., *J. Colloid Interface Sci.* **94,** 179 (1983).
51. Jokela, P., Jonsson, B., and Wennerstrom, H., *Prog. Colloid Polym. Sci.* **70,** 17 (1985).
52. Jonsson, B., and Wennerstrom, H., *J. Colloid Interface Sci.* **80,** 482 (1981).
53. Dubin, P. L., and Davis, D., *Colloids Surf.* **13,** 113 (1985).
54. Matheson, K. L., *J. Amer. Oil Chem. Soc.* **62,** 1269 (1985).